17β-Estradiol Inhibits Apoptotic Cell Death of Oligodendrocytes by Inhibiting RhoA-JNK3 Activation after Spinal Cord Injury

Jee Y. Lee, Soo Y. Choi, Tae H. Oh, and Tae Y. Yune

Age-Related and Brain Diseases Research Center (J.Y.L., T.H.O., T.Y.Y.), Neurodegeneration Control Research Center (J.Y.L., T.Y.Y.), and Department of Biochemistry and Molecular Biology (T.Y.Y.),School of Medicine, Kyung Hee University, Seoul 130-701, Korea; and Department of Biomedical Science and Research Institute of Bioscience and Biotechnology (S.Y.C.), Hallym University, Chunchon 200-702, Korea

A delayed oligodendrocyte cell death after spinal cord injury (SCI) contributes to chronic demyelination of spared axons, leading to a permanent neurological deficit. Therefore, therapeutic approaches to prevent oligodendrocyte cell death after SCI should be considered. Estrogens are well known to have a broad neuroprotective effect, but the protective effect of estrogens on oligodendrocytes after injury is largely unknown. Here, we demonstrated that 17β-estradiol attenuates apoptosis of oligodendrocytes by inhibiting RhoA and c-Jun-N-terminal kinase activation after SCI. Estrogen receptor (ER)-α and -β were expressed in oligodendrocytes of the spinal cord, and 17β-estradiol treatment significantly inhibited oligodendrocyte cell death at 7 d after injury as compared with vehicle (cyclodextrin) control. 17β-Estradiol also attenuated caspase-3 and -9 activation at 7 d and reduced the loss of axons from progressive degeneration. In addition, 17β-estradiol inhibited RhoA and JNK3 activation, which were activated and peaked at 3 and/or 5 d after injury. Furthermore, administration of Rho inhibitor, PEP-1-C3 exoenzyme, inhibited RhoA and JNK3 activation, and decreased phosphorylated c-Jun level at 5 d after injury. Additionally, the attenuation of RhoA and JNK3 activation as well as oligodendrocyte cell death by 17β-estradiol was reversed by ER antagonist, ICI182780. Our results thus indicate that 17β-estradiol treatment improves functional recovery after SCI in part by reducing oligodendrocyte cell death via inhibition of RhoA and JNK3 activation, which were ER dependent. Furthermore, improvement of hindlimb motor function by posttreatment of 17β-estradiol suggests its potential as a therapeutic agent for SCI patients. (*Endocrinology* 153: 3815–3827, 2012)

Oligodendrocytes undergo a delayed apoptosis in the white matter (WM) tract distant from the injury site for weeks after spinal cord injury (SCI) (1–3). This secondary degenerative event in oligodendrocytes contributes to chronic demyelination of spared axons and exacerbates the extent of injury, leading to a permanent functional deficit after SCI (1, 4–7).

The mammalian Rho GTPase family consists of at least 14 different members: Rho (A, B, and C), Rac (1, 2, and 3), Cdc42, RhoD, RhoG, RhoH/TTF, TC10, and Rnd (1, 2, and 3) (8). Rho GTPases act as intracellular molecular switches that transduce extracellular signals to the actin cytoskeleton. Rho GTPases are also involved in neuronal morphogenesis, axon growth and guidance, dendrite development, plasticity, and synapse formation (9). In addition, Rho activation is known to block axon regeneration and participate in cell death after SCI (10). Especially, RhoA activation after SCI is involved in oligodendrocyte

Abbreviations: DAPI, 4′,6-Diamidino-2-phenylindole; DMSO, dimethylsulfoxide; ER, estrogen receptor; FG, fluorogold; FITC, fluorescein isothiocyanate; GFAP, glial fibrillary acidic protein; GM, gray matter; GST, glutathione S-transferase; JNK, c-Jun N-terminal kinase; LVe, lateral vestibular nucleus; MBP, myelin basic protein; MdV, ventral medullary reticular formation; NeuN, neuronal nuclei; p-c-Jun, phosphorylated c-Jun; PnC, caudal pontine reticular formation; RBD, Rho-binding protein domain; RN, red nucleus; SCI, spinal cord injury; TUNEL, terminal deoxynucleotidyl transferase-mediated deoxyuridine triphosphate-biotin nick end labeling; WM, white matter.

apoptosis via p75 neurotrophin receptor activation (11, 12). Therefore, RhoA appears to be a potential therapeutic target protein in view of promoting axonal repair after SCI.

The c-Jun N-terminal kinase (JNK) pathways typically are activated by proinflammatory as well as various stress signals in the nervous system (13). JNK3, one isoform of three JNK (JNK1, -2, and -3), is selectively expressed in the nervous system (14) and is implicated in the apoptotic cell death under a wide range of pathological conditions, such as ischemia (15, 16), axotomy (17, 18), and seizure (19) and in animal models of neurodegenerative diseases (20, 21). Recent evidence also shows that JNK3 activity is increased and sustained in a prolonged manner until several days after SCI, and apoptotic cell death of oligodendrocytes is reduced in JNK3$^{-/-}$, suggesting that the JNK3 pathway is involved in oligodendrocyte cell death after SCI (22).

Estrogens can be a potential therapeutic agent for the treatment of many neurodegenerative diseases such as Alzheimer's disease, Parkinson's disease, stroke, and brain trauma because it has a broad neuroprotective effect against a variety of insults to the central nervous system (23–26). Our previous report also shows that 17β-estradiol improves functional recovery by inhibiting apoptosis of neurons after SCI (27), which is mediated through pERK-induced cAMP response element-binding protein-dependent bcl-2 induction (28). However, the protective effect of estrogens on oligodendrocyte cell death after SCI is largely unknown. Because preservation of myelinated axons has a direct correlation with functional outcome after injury, here we examined whether 17β-estradiol exerts its protective effect on oligodendrocyte cell death after SCI and whether RhoA and JNK3 pathways are implicated in its protective effect. Our data indicate that estrogen improved functional recovery after SCI by reducing apoptotic cell death of oligodendrocytes via inhibition RhoA-JNK3 activation, which is through the estrogen receptor (ER).

Materials and Methods

Spinal cord injury

Adult male Sprague Dawley [Sam:TacN (SD) BR; Samtako, Osan, Korea] rats were subjected to moderate 25 g-cm contusion injury as described previously (12). Surgical interventions and postoperative animal care were performed in accordance with the Guidelines and Policies for Rodent Survival Surgery provided by the Animal Care Committee of the Kyung Hee University. For details on SCI, see Supplemental Methods (published on The Endocrine Society's Journals Online web site at http://endo.endojournals.org).

Oligodendrocyte culture

Primary cultures of rat cortical oligodendrocytes were prepared as described previously (12). For details on oligodendrocyte culture, see Supplemental Methods.

Drug administration

17β-Estradiol (2-hydroxypropyl-β-cyclodextrin-encapsulated; Sigma Aldrich, St. Louis, MO) was dissolved in sterile 0.1 M PBS (pH 7.4). For determination of optimal dose of 17β-estradiol, rats receiving the 25 g-cm injury received iv injections of 17β-estradiol at a dose of 100, 300, or 600 μg/kg via tail vein within 5 min after SCI and then at 6 and 24 h with the same dose; the vehicle control group received injections of cyclodextrin in PBS with the same interval. As an optimal dosage, 300 μg/kg 17β-estradiol was selected and used throughout experiments (see Fig. 8A). ER antagonist ICI182780 (Tocris Cookson, Inc., Ellisville, MO) was dissolved in 50% dimethylformamide in 0.9% saline and was given (3 mg/kg, ip) before each injection of 17β-estradiol.

Tissue preparation

At specific time points after SCI, animals were anesthetized with chloral hydrate (500 mg/kg) and perfused via cardiac puncture initially with 0.1 M PBS and subsequently with 4% paraformaldehyde in 0.1 M PBS. A 20-mm section of the spinal cord, centered at the lesion site, was dissected out, postfixed by immersion in the same fixative overnight, and placed in 30% sucrose in 0.1 M PBS. The segment was embedded in OCT for frozen sections, and longitudinal or transverse sections were then cut at 10 or 20 μm on a cryostat (CM1850; Leica, Wetzlar, Germany).

Terminal deoxynucleotidyl transferase-mediated deoxyuridine triphosphate-biotin nick end labeling (TUNEL)

Seven days after injury, serial spinal cord sections (10 μm thickness) were collected every 200 μm and processed for TUNEL staining using an Apoptag *in situ* kit (Millipore, Billerica, MA). For details, see Supplemental Methods.

Immunostaining

Frozen sections were blocked with 5% normal serum and 0.1% Triton X-100 in PBS for 1 h at room temperature and then incubated with primary antibodies of phosphorylated c-Jun (p-c-Jun) (1:100; Cell Signaling Technology, Danvers, MA), cleaved caspase-3 (1:100; Millipore), ER-α (1:100; Santa Cruz Biotechnology, Santa Cruz, CA), ER-β (1:100; Millipore), CC1 (1:100; Millipore), neuronal nuclei (NeuN), (1:200; Millipore), glial fibrillary acidic protein (GFAP) (1:5000; Millipore), OX-42 (1:100; Millipore), and myelin basic protein (MBP) (1:500; Millipore) overnight at 4 C. For double labeling, fluorescein isothiocyanate (FITC)- or Cy-3-conjugated secondary antibodies (Jackson Laboratories, Danvers, MA) were used. Also, nuclei were labeled with 4′,6-diamidino-2-phenylindole (DAPI) according to the protocol of the manufacturer (Invitrogen, Carlsbad, CA). In all immunohistochemistry controls, reaction to the substrate was absent if the primary antibody was omitted or if the primary antibody was replaced with a nonimmune, control antibody. Some serial sections were also stained with cresyl violet acetate for histological analysis. For quantification of p-c-Jun-positive neurons or oligodendrocytes, serial transverse sections (10 μm thickness) were collected every 100 μm from 8 mm rostral to 8 mm caudal to the lesion epicenter (total 160 sections), and double-positive neurons (p-c-Jun + NeuN) in the lower ventral horn of gray matter (GM) and oligodendrocytes (p-c-Jun +

CC1) in the lateral and ventral funiculus of WM were manually counted and averaged. The quantification of cleaved caspase-3-positive oligodendrocytes (cleaved caspase-3 + CC1) was performed by same method for quantification of p-c-Jun-positive oligodendrocyte as described above.

Western blot

Segments of spinal cord (1 cm) were isolated containing the lesion site as the epicenter, and the tissue homogenates were prepared as previously described (12). Tissue homogenate was centrifuged twice at $13,000 \times g$ for 10 min at 4 C, and the protein levels of the supernatant were determined using the bicinchoninic acid assay (Pierce, Rockford, IL). For analyses by Western blot, 50 μg protein was separated by 12% SDS-PAGE and transferred to nitrocellulose membranes (Millipore) by electrophoresis. The membranes were blocked with 5% nonfat skim milk or BSA in Tris-buffered saline with 0.1% Tween 20 for 1 h at room temperature and then incubated with a primary antibodies against p-c-Jun (1:1000; Cell Signaling Technology), c-Jun, (1:500; Santa Cruz Biotechnology), cleaved caspase-3 (1:1000; Cell Signaling Technology), caspase-9 (1:500; Santa Cruz Biotechnology), JNK1/2, (1:1000; Cell Signaling Technology), His-tag (1:1000; Santa Cruz Biotechnology), RhoA (1:1000; Santa Cruz Biotechnology), ER-α (1:100; Santa Cruz Biotechnology), and ER-β (1:100; Millipore) overnight at 4 C. The membranes were then processed with horseradish peroxidase-conjugated secondary antibody (Jackson Laboratories). Immunoreactive bands were visualized by chemiluminescence using Supersignal (Pierce). Experiments were repeated three times to ensure reproducibility.

RNA isolation and RT-PCR

Total RNA isolation using Trizol reagent (Invitrogen), cDNA synthesis, and RT-PCR were performed as previously described (29). For details on RNA isolation and RT-PCR, see Supplemental Methods.

Pull-down assay for RhoA activity

Purification of glutathione S-transferase (GST)-Rho-binding protein domain (RBD) was performed as described previously (11). For details on purification of GST-RBD, see Supplemental Methods. Frozen spinal cord tissue was homogenized in a modified radioimmunoprecipitation assay buffer containing 50 mM Tris (pH 7.2), 1% Triton X-100, 0.5% sodium deoxycholate, 0.1% SDS, 500 mM NaCl, 10 mM $MgCl_2$, 10 μg/ml aprotinin, 10 μg/ml leupeptin, and 1 mM phenylmethylsulfonyl fluoride. The homogenates were clarified by centrifugation twice for 10 min at $13,000 \times g$ at 4 C. The supernatant was incubated for 50 min at 4 C with GST-RBD-coupled beads (30 μg/sample). The beads were washed four times with lysis buffer and eluted in sample buffer. GTP-bound RhoA and total RhoA present in tissue homogenates were detected by Western blot as described previously (12).

Protein kinase assay

Frozen spinal cord tissue was homogenized in a Nonidet P-40 lysis buffer. The homogenates were clarified by centrifugation twice for 10 min at $13,000 \times g$ at 4 C. The supernatant were used for kinase assay. To assay for total JNK activity (JNK1–3), tissue extracts were incubated with recombinant GST-c-jun (1–79) bound to glutathione-coupled Sepharose-beads, and [γ-^{32}P]ATP. The complex was washed extensively with lysis buffer.

Kinase activity in the complex was assayed by autoradiographic detection of labeled [γ-^{32}P]ATP. To assay for the JNK3-specific kinase activity, the cell lysates were first subjected to immunoprecipitation with the specific anti-JNK1 and -2 antibodies (Santa Cruz Biotechnology) to remove both JNK1 and JNK2 from the lysates. The remaining kinase activity (JNK3) in the supernatant was assayed by the capture JNK assay as described above. To ensure that JNK1 and -2 were completely removed from the supernatant, the supernatant was also examined by immunoblot analysis using the JNK1/2 antibody.

Axon staining and counting

At 38 d after injury, frozen sections were prepared as described above. Axons were stained using an antibody specific for 200-kDa neurofilament protein (NF200, 1:2000; Sigma). The quantitative analysis of axonal density is described in Supplemental Methods.

Retrograde tracing

Retrograde tracing using fluorogold (FG; Invitrogen) (30) was used to determine the extent to which spared descending axons reached the rostral lumbar enlargement. For details on retrograde tracing, see Supplemental Methods. The total number of FG-labeled neuronal cell bodies in selected supraspinal regions, the ventral medullary reticular formation (MdV), the lateral vestibular nucleus (LVe), the caudal pontine reticular formation (PnC), and the red nucleus (RN), was counted according to previously described methods (30). Axons from these nuclei project to the thoracolumbar spinal cord and play important roles in hindlimb locomotor function (30, 31).

Expression and administration of PEP-1-C3 protein

To introduce C3 exoenzyme (*Clostridium botulinum*) as a RhoA inhibitor into spinal cord, we fused PEP-1 sequence (KETWWETWWTEWSQPKKKRKV) to the N terminus of the C3 exoenzyme containing His-tag (32) (Supplemental Fig. 1A). The expression and purification of both recombinant PEP-1-C3 and C3 fusion protein was performed as previously described (32) (Supplemental Fig. 1, B and C). PEP-1-C3 (300 μg/kg) protein was administered by intrathecal infusion using Alzet osmotic minipump (Alzet 2001; Durect Corp., Cupertino, CA) according to manufacturer's instruction. Briefly, a mini-pump was filled with PEP-1-C3 and a catheter connected to the outlet of the mini-pump was inserted into the intrathecal space of the spinal cord at T9 through a small hole in the dura of T11–12. The tube was sutured to the spinous process just caudal to the laminectomy to anchor it in place. To examine delivery efficacy of PEP-1-C3 *in vivo*, the purified PEP-1-C3 was labeled with FITC (Pierce) according to the manufacturer's instructions and was injected intrathecally (300 μg/kg) immediately after injury. Five days after injection, spinal cord tissues were prepared and sectioned and were processed for immunohistochemical staining using specific cell type markers. The fluorescence was photographed with an Olympus microscope with software accompanying the Cool SNAP camera (Roper Scientific, Ottobrunn, Germany).

Behavioral tests

Behavioral analyses were performed according to previously described methods (33–36). For details on behavioral tests, see Supplemental Methods.

Statistical analysis

Data except behavior tests are presented as the mean ± SD values, and behavioral data are presented as the mean ± SEM. Comparisons between vehicle and 17β-estradiol-treated groups were made by unpaired Student's *t* test. Multiple comparisons between groups were performed by one-way ANOVA. Behavioral scores from Basso, Beattie, and Bresnahan analysis and inclined plane tests were analyzed by repeated-measures ANOVA (time *vs.* treatment). Tukey's multiple comparison was used as *post hoc* analysis. Statistical significance was accepted

with $P < 0.05$. All statistical analyses were performed by using SPSS version 15.0 (SPSS Science, Chicago, IL).

Results

Oligodendrocytes express ERα and -β

We first examined whether oligodendrocytes express ER-α and ER-β. First, primary oligodendrocyte cultures were prepared as described in *Materials and Methods*. As shown in Fig. 1A, differentiated oligodendrocytes expressed both ER-α and ER-β mRNA. ER-α- and ER-β-positive cells were also colocalized with MBP, an oligo-
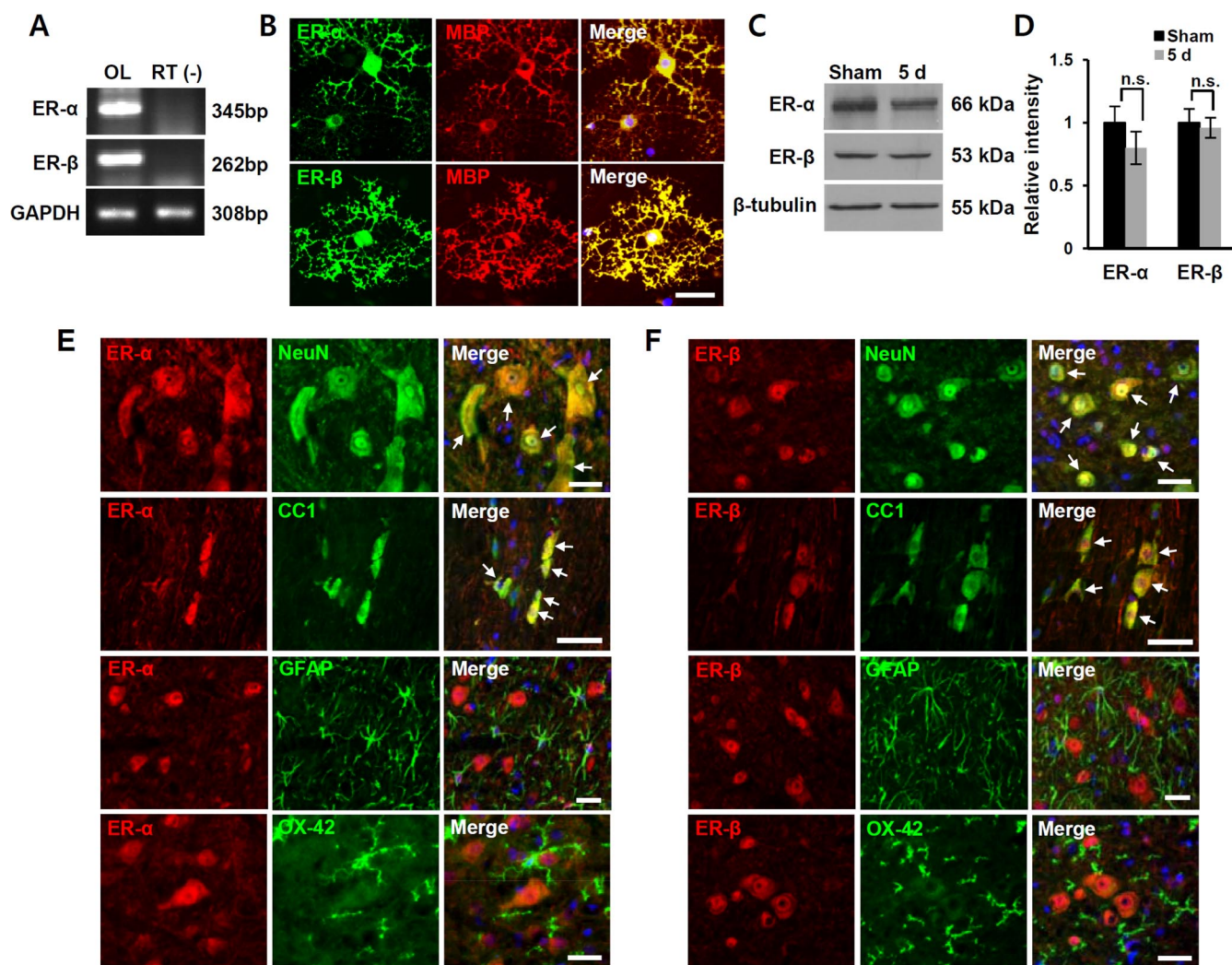
FIG. 1. Oligodendrocytes express ER-α and -β. Highly enriched oligodendrocytes were seeded on poly-D-lysine-coated six-well plates (2 × 10⁵ cells per well) and cultured for 4–5 d. A, ER-α and -β mRNA expression in differentiated oligodendrocyte cultures. B, Cultured MBP-positive oligodendrocytes express ER-α and -β. Data were obtained from three separate experiments. *Scale bar*, 20 μm. C, Western blots of ER-α and -β with total lysates from sham and injured (5 d) spinal cord. D, Densitometric analysis of Western blots. The levels of ER-α and -β expression were not changed after injury. Data are mean ± SD (n = 3). n.s., Not significant *vs.* sham control. E and F, Longitudinal sections containing ventral horn from uninjured spinal cord were processed for double staining with antibodies against ER-α and -β and cell type-specific markers (NeuN for neuron, CC1 for oligodendrocyte, GFAP for astrocyte, and OX-42 for microglia). Note that ER-α (D) and -β (E) were expressed in neurons and oligodendrocytes but not in astrocytes and microglia. *Arrows* indicate ER-positive neurons and oligodendrocytes. *Scale bars*, 50 μm. OL, Oligodendrocytes; RT, reverse transcription; ER, estrogen receptor.

dendrocyte cell-specific marker (Fig. 1B). Next, to examine ER-α and ER-β expression in the spinal cord, total lysates were prepared from sham and injured spinal cord (at 5 d). Both ER-α and ER-β were expressed in the uninjured spinal cord (Fig. 1, C and D), whereas the levels were not changed after SCI. When we performed Western blot for ER-β, the antibody strongly recognized an approximately 53-kDa signal, although several signals were faintly detected. When the membrane was stripped and reprobed with ER-β antibody after preabsorption to its corresponding peptide, the expected ER-β band (53 kDa) was greatly diminished, whereas the intensity of other bands did not change, indicating that the 53-kDa signal was specific for ER-β. To identify the cell types, we performed double immunostaining with antibodies against ER-α and ER-β and the cell-type-specific markers NeuN for neurons, CC1 for oligodendrocytes, GFAP for astrocytes, and OX-42 for microglia. As shown in Fig. 1, E and F, double labeling showed that in the uninjured normal spinal cord, neurons in the GM and oligodendrocytes in the WM were positive for both ER-α and ER-β.
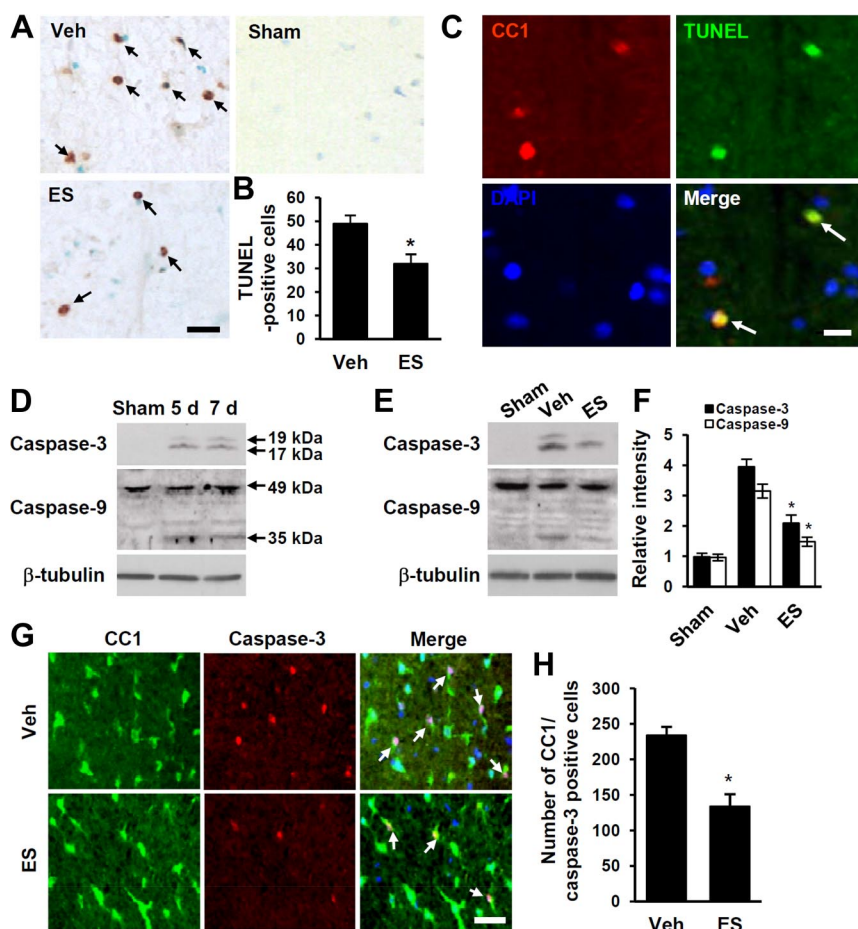
FIG. 2. 17β-Estradiol inhibits oligodendrocyte cell death after SCI. Rats receiving the 25 g-cm injury were treated with 17β-estradiol. At 7 d after injury, spinal cord sections were prepared and processed for TUNEL staining and double labeling using CC1 antibody. Representative images were from the sections selected 6 mm rostral to the lesion epicenter. A and B, TUNEL staining (A) and quantification of TUNEL-positive cells (B) in the WM. *Scale bar*, 50 μm. Data are mean $\pm$ SD (n = 5). *, $P < 0.05$ (Student's t test) *vs.* vehicle-treated control. C, Spinal cord section (transverse sections) at 6 mm rostral to the injury epicenter was stained with triple labeling with CC1 in *red*, TUNEL in *green*, and DAPI in *blue*. *Arrows* indicate TUNEL-positive oligodendrocytes. *Scale bar*, 10 μm. D and E, Western blots of caspase-3 and -9 at 5 and 7 d after injury (D) and the effect of 17β-estradiol on its activation at 7 d (E). F, Densitometric analysis of Western blots. Data are mean $\pm$ SD (n = 3). *, $P < 0.05$ (ANOVA) *vs.* vehicle-treated control. G, Double labeling of transverse spinal cord sections with cleaved (activated) caspase-3 and CC1 antibodies. Representative images were from the sections selected 5 mm rostral to the lesion epicenter. *Arrows* indicate caspase-3/CC1-positive cells. *Scale bar*, 20 μm. H, Quantitative analysis of caspase-3/CC1-positive cells in 17β-estradiol- and vehicle (cyclodextrin)-treated spinal cords at 7 d after SCI. Data are mean $\pm$ SD (n = 5). *, $P < 0.05$ (Student's t test) *vs.* vehicle-treated control. ES, 17β-Estradiol; Veh, vehicle.

17β-Estradiol attenuates apoptosis of oligodendrocytes after SCI

It is well known that estrogens exhibits neuroprotective effects against a variety of neurodegenerative diseases such as Alzheimer's disease, Parkinson's disease, stroke, and brain trauma (23–26). Our previous report also shows that 17β-estradiol improves functional recovery after SCI by inhibiting apoptotic cell death of neurons via increasing cAMP response element-binding protein-dependent bcl-2 expression (27, 28). However, the protective effect of estrogens on oligodendrocyte cell death after SCI has not been examined. Thus, we hypothesized that 17β-estradiol would inhibit oligodendrocyte cell death after SCI. Rats received iv injections of 17β-estradiol (300 μg/kg), which is the most effective dose (see Fig. 8A), 5 min and 6 and 24 h after injury with the same dose; the vehicle control group received injections of cyclodextrin in PBS with same interval. Seven days after injury, quantification of TUNEL-positive cells showed that 17β-estradiol administration reduced apoptotic cell death in the WM compared with vehicle control (Fig. 2, A and B) (17β-estradiol, 32 $\pm$ 4.0 *vs.* vehicle, 49 $\pm$ 3.5). By double staining, many of these TUNEL-positive cells were positive for an oligodendrocyte-specific marker, CC1 (Fig. 2C). More TUNEL-positive cells were observed from rostral to caudal from the lesion epicenter (data not shown). No signal was observed in sham-operated animals (Fig. 2A).

17β-Estradiol inhibits caspase-3 and -9 activation after SCI

Because 17β-estradiol inhibits apoptotic cell death of oligodendrocyte (see Fig. 2, A–C), and several reports also show that caspase-3 and -9 are activated and involved in delayed oligodendrocyte apoptosis after SCI (37–39), we expected that 17β-estradiol might inhibit caspase-3 and -9 activations after SCI. By Western blot, caspase-3 and -9 were activated at 5 and 7 d (Fig. 2D) as reported previously (38), and 17β-estradiol treatment significantly inhibited their activation when compared with vehicle control (Fig. 2, E and F) (caspase-3: estradiol, 2.09 ± 0.27 *vs.* vehicle, 3.95 ± 0.25; caspase-9: estradiol, 1.48 ± 0.15 *vs.* vehicle, 3.15 ± 0.23). By double immunostaining of cross-sections at 7 d, caspase-3/CC1-positive oligodendrocytes was increased rostrally and caudally to the epicenter (Fig. 2G). Counting of double-positive cells (caspase-3/CC1) revealed that 17β-estradiol significantly reduced the numbers of caspase-3/CC1-positive oligodendrocytes compared with vehicle control (Fig. 2H) (estradiol, 234 ± 12 *vs.* vehicle, 134 ± 17).

17β-Estradiol inhibits RhoA activation after SCI

Because RhoA activation is known to be involved in axonal degeneration (40) and in oligodendrocyte cell death after SCI (11, 12, 41), we hypothesized that 17β-estradiol would inhibit RhoA activation after SCI. RhoA activation by Rho pull-down assay was evaluated by probing tissue extracts with the RBD from the Rho-GTP-interacting protein rhotekin as described in *Materials and Methods*. The level of GTP-bound RhoA was increased and peaked at 5 d after SCI as reported (12) (see Fig. 4, A and B). Expression levels of total RhoA, as detected by Western blots from tissue extracts used for isolation of GTP-RhoA, was not changed (Fig. 3A). Furthermore, 17β-estradiol significantly inhibited RhoA activation when compared with vehicle control at 5 d (Fig. 3, C and D) (estradiol, 1.03 ± 0.04 *vs.* vehicle, 0.43 ± 0.07).

17β-Estradiol inhibits JNK3 activation and c-Jun phosphorylation

JNK3 activation has been shown to be involved in oligodendrocyte apoptosis through c-Jun phosphorylation (42, 43). Moreover, recent evidence shows that after SCI, JNK3 activation is implicated in predominantly oligodendrocyte apoptosis but not in neuronal cell death (22). Thus, we postulated that after SCI, 17β-estradiol would protect oligodendrocytes by inhibiting JNK3 activity. To assess JNK3-specific activity, JNK1 and -2 isoforms were immunodepleted with antibodies against JNK1 and -2. After depletion, there was very little or no JNK1 and -2 protein remaining as judged by Western blot with anti-
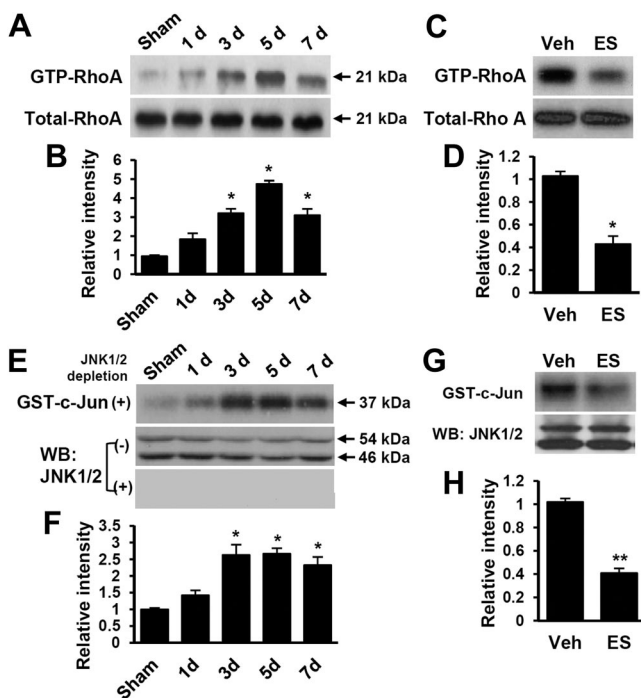
FIG. 3. 17β-Estradiol inhibits RhoA and JNK3 activation after SCI. Spinal cord extracts at indicated time points after injury were prepared and GTP-bound RhoA was isolated by pull-down assay and detected with specific antibodies against RhoA. A, RhoA is activated and peaked at 5 d after SCI and decreased thereafter. B, Densitometric analysis of Western blots. Data are mean $\pm$ SD (n = 5). *, $P < 0.05$ (ANOVA) *vs.* sham control. C and D, Effect of 17β-estradiol on RhoA activation at 5 d after SCI by Western blots (C) and densitometric analysis of Western blots (D). Data are mean $\pm$ SD (n = 5). *, $P < 0.05$ (Student's *t* test) *vs.* vehicle-treated control. E and F, JNK3 activity is increased after injury. JNK3-specific activity was measured by immunoprecipitation/kinase assay using GST-c-Jun as the substrate as described in *Materials and Methods*. Western blots (E) and densitometric analysis of Western blots (F) of JNK3 activity are shown. Data are mean $\pm$ SD (n = 5). *, $P < 0.05$ (ANOVA) *vs.* sham control. G and H, Effect of 17β-estradiol on JNK3 activation at 5 d after SCI by Western blots (G) and densitometric analysis of Western blots (H). Data are mean $\pm$ SD (n = 5). **, $P < 0.01$ (Student's *t* test) *vs.* vehicle-treated control. ES, 17β-Estradiol; Veh, vehicle; WB, Western blot.

body against JNK1/2 (Fig. 3E). Therefore, the residual JNK activity could represent JNK3 activation. The measured JNK3 activity was increased and peaked at 3–5 d after injury (Fig. 3, E and F). Furthermore, 17β-estradiol significantly reduced the JNK3 activation at 5 d when compared with vehicle control (Fig. 3, G and H) (estradiol, 0.41 ± 0.07 *vs.* vehicle, 1.02 ± 0.03). By contrast, JNK1/2 expression was not changed by 17β-estradiol (Fig. 3G).

The phosphorylation of c-Jun by JNK3 is also implicated in neuronal and oligodendroglial cell death in cerebral hypoxic-ischemic brain injury (44) and SCI (22). As a downstream activator of JNK3, we anticipated that 17β-estradiol would also reduce the level of p-c-Jun after SCI. There was little expression of p-c-Jun in sham-operated controls. However, injury to the spinal cord caused early increase of p-c-Jun level at 1 d (Fig. 4, A and B) as reported
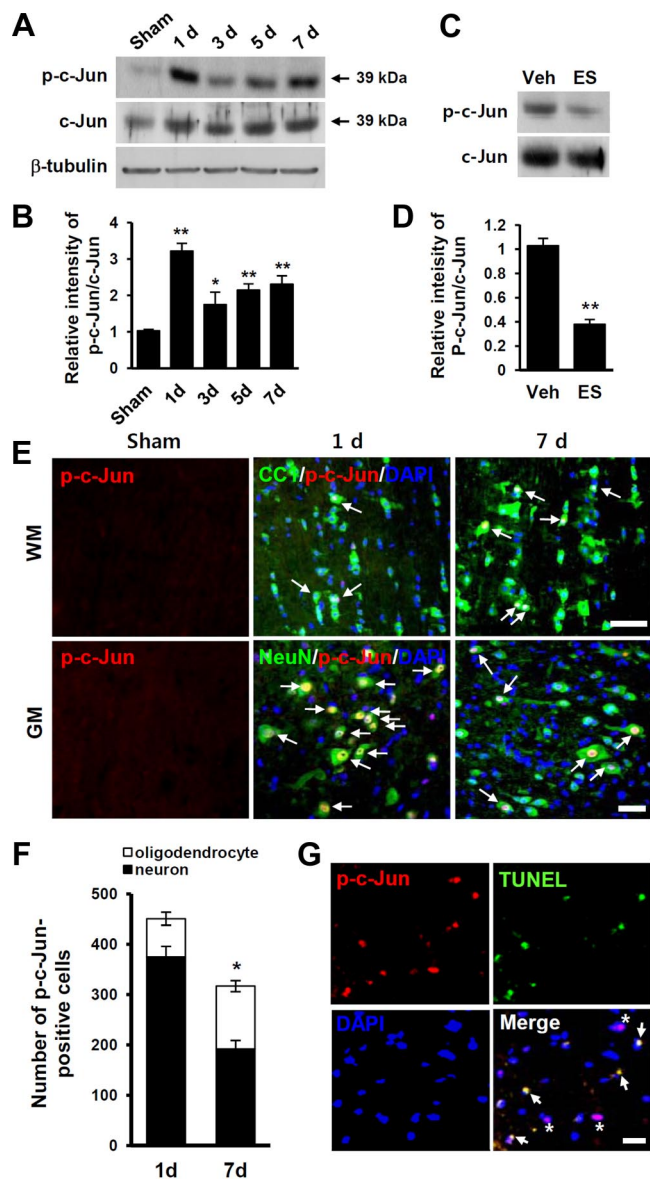
FIG. 4. 17β-estradiol inhibits c-Jun phosphorylation after SCI. Spinal cord extracts and sections were prepared at indicated time points after injury for Western blot, TUNEL and immunofluorescence staining using anti-c-Jun and anti-p-c-Jun antibodies. A and B, The levels of c-Jun and p-c-Jun after injury, shown by Western blots of c-Jun and p-c-Jun (A) and densitometric analysis of p-c-Jun (B). Data are mean ± SD (n = 3). *, P < 0.05; **, P < 0.01 (ANOVA) vs. sham control. C and D, Effect of 17β-estradiol on p-c-Jun at 7 d after injury, shown by Western blots (C) and densitometric analysis of blots (D). Data are mean ± SD (n = 3). **, P < 0.01 (Student's t test) vs. vehicle-treated control. E, Double labeling of p-c-Jun with NeuN or CC1 at 1 and 7 d after injury. Arrows indicate p-c-Jun/NeuN- or CC1-positive cells. Representative images were from the sections selected 2 mm (1 d) or 6 mm (7 d) rostral to the lesion epicenter. Scale bar, 20 μm. F, Quantification of mean number of p-c-Jun-positive neurons and oligodendrocytes at 1 and 7 d after SCI. Data are mean ± SD (n = 5). *, P < 0.05 (Student's t test) vs. 1 d. G, TUNEL-positive cells colocalized with p-c-Jun at 7 d after injury. Transverse spinal cord sections at 6 mm rostral to the injury epicenter was stained with triple labeling with p-c-Jun in red, TUNEL in green, and DAPI in blue. Arrows indicate p-c-Jun/TUNEL-positive cells in the WM. Asterisks indicate p-c-Jun-positive cells with negative TUNEL signal. Scale bar, 20 μm. ES, 17β-Estradiol; Veh, vehicle.

(45). At delayed time points (at 5–7 d), the level of p-c-Jun was also increased (Fig. 4, A and B). Furthermore, 17β-estradiol significantly reduced the level of p-c-Jun compared with vehicle control (Fig. 4, C and) at 7 d (estradiol, 0.38 ± 0.04 vs. vehicle, 1.03 ± 0.06). These results were also confirmed with double immunohistochemical detection and counting the number of p-c-Jun-positive cells at 1 and 7 d. In contrast to sham controls, which showed no p-c-Jun-positive signal (Fig. 4E, Sham), intense signals for p-c-Jun were detected in neurons and oligodendrocytes at 1 and 7 d (Fig. 4E). When p-c-Jun-positive cells were counted and analyzed at 1 d, most p-c-Jun immunoreactivity was detected in neurons in the GM. However, the number of p-c-Jun-positive oligodendrocytes was increased 2.5-fold at 7 d when compared with that at 1 d, whereas the number of p-c-Jun-positive neurons was decreased (Fig. 4, E and F). Next, to investigate whether c-Jun phosphorylation might be involved in apoptotic cell death of oligodendrocytes, TUNEL staining was performed with immunostaining with p-c-Jun antibody using spinal tissues from 7 d. As shown in Fig. 4G, many p-c-Jun-positive oligodendrocytes in the WM were positive for TUNEL, indicating that c-Jun phosphorylation is involved in the apoptotic cell death of oligodendrocytes at 7 d after SCI.

17β-Estradiol prevents axonal loss after SCI

It is known that axonal loss via wallerian degeneration and axon dieback occurs after SCI (46, 47). In addition, inactivation of Rho or its downstream target Rho-associated kinase (ROCK) is known to promote central nervous system axon regeneration of crushed optic nerves in adult rats (48) and stimulates axon regeneration after SCI, leading to recovery of hindlimb function (49). Furthermore, our data showed that 17β-estradiol inhibited RhoA activation after injury (see Fig. 3C). Thus, we hypothesized that 17β-estradiol would reduce axonal loss after SCI. When we counted the number of NF200-positive axons in the preselected areas of the WM after staining with NF200 using cross-sections from at 38 d after injury, we observed that axon loss occurred rostrally and caudally from the lesion epicenter (Fig. 5, A and B). However, 17β-estradiol treatment markedly reduced the extent of axon loss compared with vehicle control (Fig. 5, A and B). Next, we performed retrograde tracing to assess the extent of spared or regenerated descending axons using a retrograde tracer, FG. Notably, the mean number of FG-labeled neurons in selected supraspinal nuclei in the brain was significantly higher in the 17β-estradiol-treated group than in vehicle control (Fig. 5, C and D). They were MdV/MdD (vehicle, 502 ± 23 vs. estradiol, 702 ± 33), Lve (vehicle, 98 ± 15 vs. estradiol, 2030 ± 12), PnC (vehicle, 132 ± 22 vs. es-
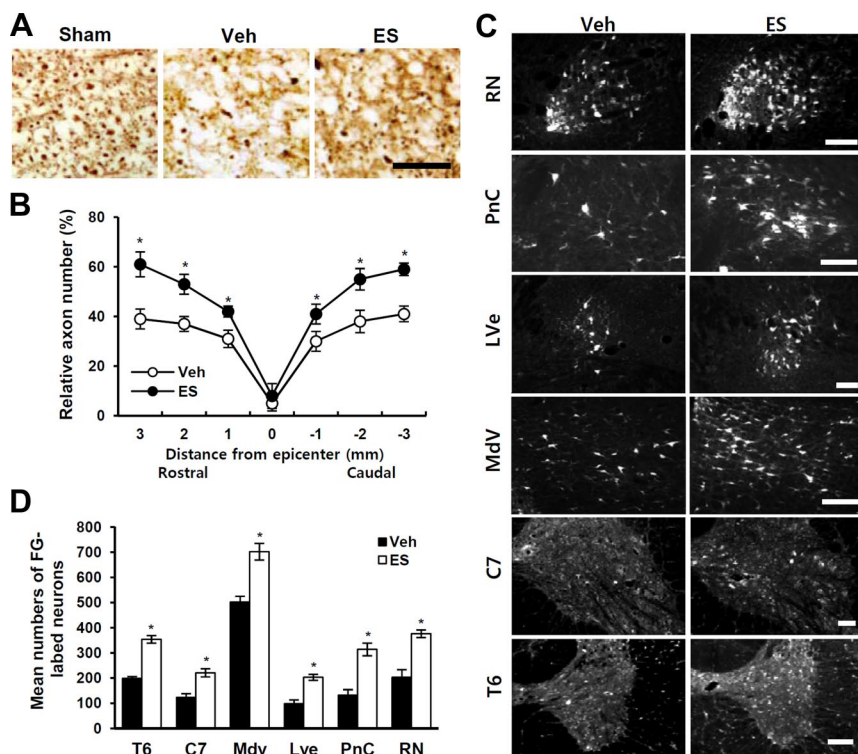
FIG. 5. 17β-Estradiol reduces axon loss after SCI. After behavioral tests, spinal cords at 38 d after injury were processed and transverse cryosections were selected 3 mm rostrocaudal to the lesion site for neurofilament staining with NF200 antibody. A, Axon loss occurred after SCI compared with sham control. The number of NF-positive axons in the 17β-estradiol-treated group was higher than that in the vehicle (cyclodextrin)-treated group. *Scale bar*, 30 μm. B, Quantitative analysis of neurofilament-stained axons within the vestibulospinal tract shows that the number of axons in the 17β-estradiol-treated groups was significantly higher than in the vehicle groups. Data are mean ± SD (n = 5). *, $P < 0.05$ (ANOVA) *vs.* vehicle-treated control. C, Axonal transport and/or axon sparing is increased by 17β-estradiol after SCI. FG was applied to rats tested for behavior at the L1 site, and at 7 d after FG treatment, spinal and brain sections were prepared. Note that the number of FG-labeled neurons both in propiospinal (T6 and C7) and in four brainstem regions, MdV, LVe, PnC, and RN, was higher in 17β-estradiol-treated groups than in vehicle-treated groups. *Scale bar*, 100 μm. D, Quantification of FG-labeled neurons in spinal cord and brainstem. Data are mean ± SD (n = 5). *, $P < 0.05$ (Student's *t* test) *vs.* vehicle-treated control. ES, 17β-Estradiol; Veh, vehicle.

tradiol, 314 ± 25), and RN (vehicle, 203 ± 30 *vs.* estradiol, 376 ± 15).

RhoA activation mediates JNK3 activation after SCI

Our data showed that both RhoA and JNK3 were activated at a delayed time after injury, and estrogen significantly attenuated RhoA and JNK3 activation, leading to inhibition of oligodendrocyte cell death. Next, to examine the role of RhoA activation in oligodendrocyte cell death and the relationship between RhoA and JNK3, we constructed the expression vector of PEP-1-exoenzyme C3 (PEP-1-C3) fusion protein to use as an inhibitor for RhoA (Supplemental Fig. 1, A and B), which can be inactivated by ADP ribosylation via C3 transferase of *C. botulinum* (50). PEP-1-C3 proteins were purified and further confirmed with matrix-assisted laser desorption/ionization-time of flight mass spectrometry (data not shown) and

Western blot with antibody against His-tag for protein identification (Supplemental Fig. 1C). To investigate the ability of PEP-1-C3 protein to transduce into cells, matured oligodendrocyte cultures were incubated with PEP-1-C3 (10 and 50 μg/ml) for indicated time periods. As shown in Supplemental Fig. 1, D and E, PEP-1-C3 effectively entered into oligodendrocytes, and the level peaked at 3 h after incubation. To examine the delivery efficacy of PEP-1-C3 in the spinal cord, PEP-1-C3 (300 μg/kg) was labeled with FITC and intrathecally injected into the cord. Locally infused PEP-1-C3-FITC was also effectively transduced into neurons, oligodendrocytes, astrocytes, and microglia (Supplemental Fig. 1F).

Next, we examined the effect of PEP-1-C3 on RhoA activation and oligodendrocyte cell death after SCI. As shown in Fig. 6, A and B, transduced PEP-1-C3 significantly inhibited RhoA activation at 5 d after SCI compared with vehicle control (C3), which was not transduced into the spinal cord tissue as in our previous report (51). In addition, the number of TUNEL-positive oligodendrocytes was significantly reduced in the PEP-1-C3-treated group compared with the vehicle group (C3, 53 ± 5 *vs.* PEP-1-C3, 36 ± 3) (Fig. 6C). To investigate the relationship between RhoA and JNK3, we also assayed JNK3 activity and the level of p-c-Jun after PEP-1-C3 treatment. As shown in Fig. 6, D and E, both JNK3 activity and the level of p-c-Jun at 5 d after injury were significantly decreased by PEP-1-C3 when compared with vehicle (C3) control.

17β-Estradiol inhibits RhoA and JNK3 activation via ER

To examine whether the inhibition of SCI-induced RhoA and JNK3 activation and oligodendrocyte cell death by 17β-estradiol might be mediated through ER, we employed ICI182780, an ER antagonist. It has been reported that ER-α has a 7-fold and ER-β has a 3-fold greater relative affinity to ICI182780 than to 17β-estradiol (52). After SCI, ICI182780 (3 mg/kg) was injected ip before 17β-estradiol treatment, and GTP-bound RhoA level and JNK3 activity were measured. As shown in Fig.
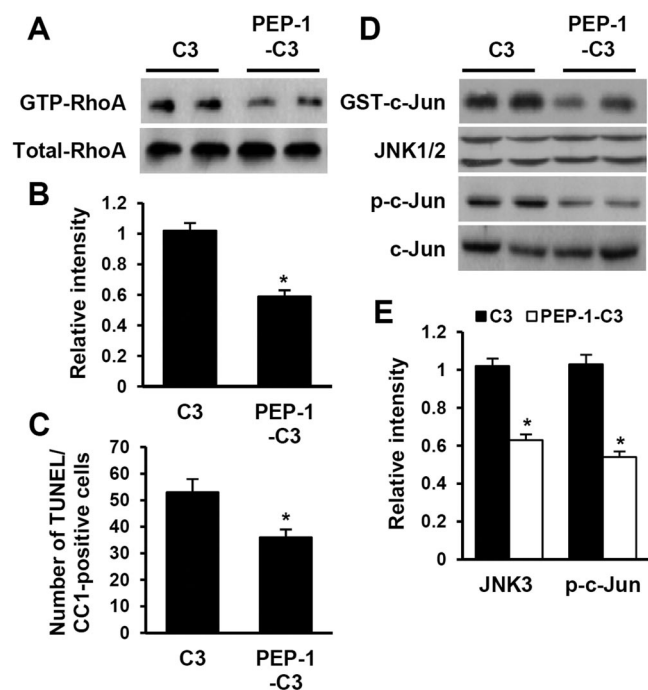
FIG. 6. PEP-1-C3 inhibits RhoA and JNK3 activation after SCI. Five days after PEP-1-C3 infusion (300 μg/kg) into injured rats, total protein was extracted and analyzed for RhoA and JNK3 activity. A, Infusion of PEP-1-C3 significantly inhibited RhoA activation after SCI compared with C3-treated control. Active GTP-RhoA was isolated by pull-down assay and detected with antibodies specific for RhoA. B, Densitometric analysis of RhoA Western blots. C, PEP-1-C3 significantly reduced the number of TUNEL-positive cells in the WM at 5 d after SCI when compared with C3-treated control. D and E, JNK3 activity (D, *upper*)/ Western blot of p-c-Jun (D, *bottom*) and densitometric analysis of Western blots (E) show that PEP-1-C3 significantly inhibited JNK3 activation and c-Jun phosphorylation at 5 d after SCI compared with C3-treated control. All data are mean ± SD (n = 5). *, $P < 0.01$ (Student's *t* test) *vs.* C3-treated control.

FIG. 7. ICI182780, an estrogen antagonist, reverses the protective effects of 17β-estradiol on RhoA and JNK3 activation and oligodendrocyte cell death after SCI. Injured rats were administered with ER antagonist ICI182780 (3 mg/kg) ip before 17β-estradiol treatment. At 5 d after injury, spinal cord sections and total extracts were prepared and subjected to RhoA and JNK3 activity assay. A, The inhibitory effects of 17β-estradiol on RhoA and JNK3 activation after injury were reversed by ICI182780 treatment. B, Densitometric analyses of Western blots of RhoA and JNK3 activation. C, ICI182780 alone did not affect on RhoA and JNK3 activation. D, The decreased number of TUNEL-positive cells by 17β-estradiol after injury was reversed by ICI182780 treatment. All data are mean ± SD (n = 5). *, $P < 0.05$ (ANOVA) *vs.* estrogen/DMSO-cotreated group. ES, 17β-Estradiol; ICI, ICI182780; Veh, vehicle.

7, A and B, ICI182780 reversed the effects of 17β-estradiol on RhoA and JNK3 activation after SCI. ICI182780 alone did not have an affect on RhoA and JNK3 activation (Fig. 7C). In addition, the reduction in the number of TUNEL/ CC1-positive cells by 17β-estradiol after SCI was also reversed by ICI182780 [estradiol + dimethylsulfoxide (DMSO), 37 ± 3.3 *vs.* estradiol + ICI182780, 52 ± 2] (Fig. 7D).

Therapeutic dosage and time windows for 17β-estradiol treatment after SCI

We previously showed that 17β-estradiol treatment 1–2 h before and immediately after SCI improves functional recovery of hindlimb locomotion (27). Therefore, it is indispensable to determine the dosage and time windows of 17β-estradiol treatment for behavioral improvement in view of therapeutic approaches. After moderate (25 mm) SCI, 17β-estradiol (100, 300, and 600 μg/kg) was administered as described in *Materials and Methods* and examined the effect on functional recovery. As shown

in Fig. 8A, BBB scores were significantly increased in 300- and 600-μg/kg 17β-estradiol-treated groups when compared with vehicle control, whereas 100-μg/kg 17β-estradiol-treated groups showed no significant effect. To determine the time windows of 17β-estradiol, rats were divided into four groups (group 1, 2 h; group 2, 6 h; group 3, 12 h to first injection of 17β-estradiol after injury; and vehicle-treated control group), and functional recovery was assessed by BBB test, inclined plane test, footprint analysis, and grid walk test. As shown in Fig. 8B, 17β-estradiol treatment significantly increased BBB scores in either 2 or 6 h, whereas no significant effect was observed in the 12-h-after-injury group compared with vehicle control group. The angle capacity to sustain was also significantly higher in rats administered 17β-estradiol 2 and 6 h after injury when compared with vehicle control (Fig. 8C). After SCI, the degree of footfall frequency increased; for example, about 60% of footfall per total steps was observed in vehicle-treated rats. However, the grid error percentage in groups administered after a 2- and 6-h delay was significantly lower than that observed in vehicle control groups (Fig. 8D). The representative footprint recordings also showed that rats treated with 17β-estradiol
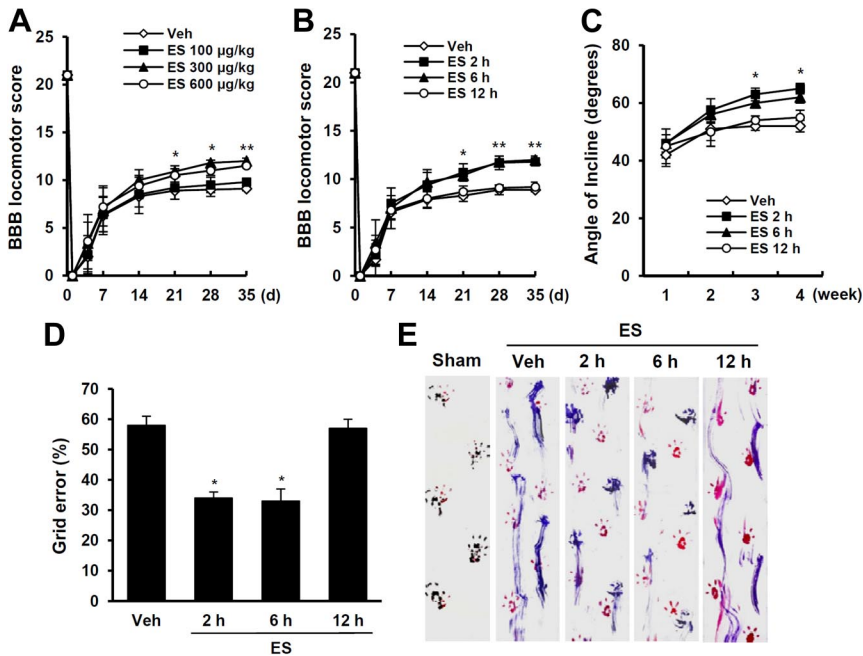
FIG. 8. Therapeutic dosage and time windows for 17β-estradiol treatment after SCI. To determinate the optimal dose, 17β-estradiol (100, 300, and 600 μg/kg) or vehicle (cyclodextrin) was administered immediately after injury and then again at 6 and 24 h. Functional recovery was assessed by BBB test. A, BBB score was significantly improved in 300- and 600-μg/kg 17β-estradiol-treated groups when compared with vehicle groups, whereas 100-μg/kg 17β-estradiol-treated groups showed no significant effect. To determine the therapeutic time windows, 17β-estradiol (300 μg/kg) was treated at 2, 6, or 12 h after injury and then further treated at 6 and 24 h. Functional improvement was assessed by BBB score (B), inclined plane test (C), grid walk test (D), and footprint analysis (E). Note that 17β-estradiol treatment (after 2- or 6-h delay) significantly improved BBB score and reduced an error percentage in grid walk test when compared with vehicle control. However, 17β-estradiol treatment after a 12-h delay showed no significant effect on recovery. Representative footprints showed that 17β-estradiol treatment (after 2- or 6-h delay) improved foot coordination, whereas rats treated with vehicle and 17β-estradiol at 12 h after injury showed inconsistent coordination and toe dragging. All data are mean ± SEM (n = 10). *, $P < 0.05$; **, $P < 0.01$ (ANOVA) *vs.* vehicle-treated control. ES, 17β-Estradiol; Veh, vehicle.

within 2 and 6 h after injury had very little toe dragging and even fairly constant forelimb-hindlimb coordination (Fig. 8E), whereas toe dragging and inconstant forelimb-hindlimb coordination were observed in vehicle control and 17β-estradiol-treated group at 12 h after injury. On the other hand, consistent forelimb-hindlimb coordination, no toe dragging, and no paw rotation were observed in sham control.

Discussion

Here we report that 17β-estradiol protects oligodendrocytes from apoptotic cell death occurred after SCI by inhibiting RhoA and JNK3 activation, which are known to be involved in oligodendrocyte cell death after SCI (11, 22). Furthermore, we first provide evidence that RhoA activation plays as an upstream activator for JNK3 phosphorylation after SCI. By inhibiting RhoA activation by

17β-estradiol or PEP-1-C3 (RhoA inhibitor) after SCI, both JNK3 activation and the level of p-c-Jun were decreased. We also found that the inhibition of RhoA and JNK3 activation by 17β-estradiol, thereby reducing oligodendrocyte cell death after SCI, was mediated through ER-α and/or -β. Finally, we provide therapeutic dosage (300 μg/kg) and time windows (2 and 6 h after injury) for 17β-estradiol treatment after SCI in the rat.

Our data showed that 17β-estradiol significantly inhibited oligodendrocyte cell death and axon loss in the WM after SCI (see Figs. 2 and 6). Rho activation after SCI has been implicated in axonal degeneration (40), and the inhibition of Rho or Rho kinase, an effecter of Rho, is known to promote axonal regeneration and functional recovery after SCI (49, 53). RhoA activation is also involved in apoptotic cell death of neurons and oligodendrocytes after SCI (11). Our study showed that RhoA was activated after SCI, and 17β-estradiol significantly inhibited RhoA activation (see Fig. 3, A–D). In addition, apoptotic cell death of oligodendrocytes after SCI was significantly inhibited by PEP-1-C3, a RhoA inhibitor (see Fig. 6, D and E). Furthermore, our previous report also shows that minocycline inhibits oligodendrocyte cell death by alleviating RhoA activation after SCI (12). Taken together, our results suggest that the inhibition of oligodendrocyte cell death and axon loss by 17β-estradiol appears to be mediated by inhibition of RhoA activation after SCI.

Generally, estrogens are known to exert its effects via ER-dependent or -independent mechanisms (54–57). It is considered that physiological levels of 17β-estradiol act through genomic mechanisms to protect neurons against ischemic insults (56, 58), whereas the supraphysiological concentrations or pharmacological levels of estrogen act through nongenomic mechanisms such as by antioxidant activity (26, 59). In this study, the pharmacological level of 17β-estradiol was used. Thus, we suspect that the protective effect of 17β-estradiol on oligodendrocyte cell death and functional improvement after SCI may be mediated through a nongenomic pathway. However, our data also showed that both ER-α and -β were expressed in both oligodendrocytes and neurons, and the attenuation

of RhoA and JNK3 activation by 17β-estradiol was processed via ER-α and/or -β-mediated signaling because ICI182780 reversed the inhibitory effect by 17β-estradiol (see Fig. 7, A and B). Furthermore, several ER-dependent mechanisms via modulation of the Bcl-2 family (56, 60), activation of phosphatidylinositol 3-kinase (57), MAPK (61), and induction of heat-shock proteins have been reported (62). Thus, we cannot rule out the possibility that ER-dependent mechanisms may also contribute to the inhibition of RhoA and JNK3 activation by 17β-estradiol.

Little is known regarding which mechanisms of RhoA activation underlying apoptotic cell death are involved. In this regard, only the facts that after serum deprivation, caspase-3 is required for Rho-mediated apoptosis (63, 64) and the activation of the JNK pathway can also occur in response to Rho activation (65) have been reported. Therefore, it is important to find the downstream signaling molecule affected by RhoA activation in apoptotic cell death of oligodendrocytes after SCI. JNK3 is known to play a preferential role in stress-induced neuronal apoptosis in brain (15, 19, 66). Furthermore, a recent report shows that JNK3 participates in oligodendrocyte apoptosis after SCI (22). Our data also show that JNK3 was activated and peaked at 3–5 d after SCI (see Fig. 3, E and F), at the time in which oligodendrocyte cell death also peaked (see Fig. 2) (12). In addition, 17β-estradiol significantly inhibited JNK3 activity, which was dependent on ER-mediated signaling (see Fig. 7, A and B). Furthermore, RhoA and JNK3 were activated at the same peak time (5 d) after SCI, and local infusion of PEP-1-C3, an inhibitor of RhoA, inhibited JNK3 activation. Thus, our results indicate that JNK3 is involved in oligodendrocyte cell death as a downstream molecule of RhoA activation, which is inhibited by 17β-estradiol (Supplemental Fig. 2).

It is well known that the phosphorylation of c-Jun occurs at an early time in degenerating and apoptotic neurons after ischemia, nerve fiber transection, UV irradiation (67), axotomy, other forms of neuronal and axonal injuries (68, 69), and traumatic brain and spinal cord injuries (45, 70, 71). According to previous reports showing that JNK1/2 activation occurs at an early time after SCI (22, 45), the phosphorylation of c-Jun at 1 d after injury in the present study appears to be the result of early JNK1/2 activation. However, the level of p-c-Jun was increased at a delayed time (7 d) as well as at an early time (1 d) after injury (see Fig. 4A). In addition, the number of p-c-Jun/CC1-positve oligodendrocytes was increased at 7 d after injury, whereas the number of p-c-Jun/NeuN-positive neurons was decreased when compared with those at 1 d after injury (see Fig. 4, E and F). These data suggest that the phosphorylation of c-Jun at a delayed time (7 d) after injury appears to be regulated by JNK3 activation after

SCI. In addition, p-c-Jun-positive oligodendrocytes were colocalized with TUNEL immunoreactivity at 7 d (see Fig. 4G), implying that the phosphorylation of c-Jun at a delayed time is involved in apoptotic cell death of oligodendrocytes. Furthermore, this late c-Jun phosphorylation was inhibited by PEP-1-C3, an inhibitor of RhoA, and 17β-estradiol (Figs. 4C and 8D). Thus, our data suggest that the inhibition of oligodendrocyte cell death by 17β-estradiol is likely mediated by inhibiting JNK3 activation followed c-Jun phosphorylation after SCI (Supplemental Fig. 2).

In this study, 17β-estradiol (100, 300, or 600 μg/kg iv) was administered at 5 min and 6 and 24 h after injury to uncastrated male rats. When the physiological level (about 30 pg/ml in plasma of male rats) of 17β-estradiol is considered (72), the dosage of 17β-estradiol used in this study is the pharmacological level. However, any significant change in body weight and side effects was not observed among the experimental groups during the experiment (data not shown). Although it is also known that testosterone can be converted into estradiol by aromatase (73), the possibility of the effect by aromatization of endogenous testosterone can be ruled out because the pharmacological level of 17β-estradiol was used in this study. Thus, we believe that the neuroprotective effects of 17β-estradiol were mainly exerted by exogenous 17β-estradiol.

Finally, we determined therapeutic dosage and time windows for 17β-estradiol treatment after SCI. Our previous report shows that in mild contusion injury (12.5 g-cm), 100 μg/kg 17β-estradiol significantly improved functional recovery (27). However, after moderate (25 g-cm injury) injury, BBB scores were significantly increased by 300 and 600 μg/kg 17β-estradiol, whereas 100 μg/kg 17β-estradiol showed no significant effect (see Fig. 8A). For time windows, functional recovery assessed by BBB score, incline test, grid walking, and footprint analysis was significantly improved in groups administered at 2 and 6 h after SCI (after treatment), whereas groups administered at 12 h after injury showed no beneficial effect (Fig. 8, B–E). Thus, the determination of therapeutic windows provides the possibility that 17β-estradiol can be used as a potential therapeutic agent for reducing oligodendrocyte cell death and axon loss, thereby improving functional recovery after SCI in humans.

Acknowledgments

10th Floor, Dongdaemun-gu, Hoegi-dong 1, Seoul 130-701, Korea. E-mail: tyune@khu.ac.kr.

References

1. **Abe Y, Yamamoto T, Sugiyama Y, Watanabe T, Saito N, Kayama H, Kumagai T** 1999 Apoptotic cells associated with Wallerian degeneration after experimental spinal cord injury: a possible mechanism of oligodendroglial death. J Neurotrauma 16:945–952

2. **Casha S, Yu WR, Fehlings MG** 2001 Oligodendroglial apoptosis occurs along degenerating axons and is associated with FAS and p75 expression following spinal cord injury in the rat. Neuroscience 103:203–218

3. **Springer JE, Azbill RD, Knapp PE** 1999 Activation of the caspase-3 apoptotic cascade in traumatic spinal cord injury. Nat Med 5:943–946

4. **Beattie MS, Harrington AW, Lee R, Kim JY, Boyce SL, Longo FM, Bresnahan JC, Hempstead BL, Yoon SO** 2002 ProNGF induces p75-mediated death of oligodendrocytes following spinal cord injury. Neuron 36:375–386

5. **Becerra JL, Puckett WR, Hiester ED, Quencer RM, Marcillo AE, Post MJ, Bunge RP** 1995 MR-pathologic comparisons of wallerian degeneration in spinal cord injury. AJNR Am J Neuroradiol 16:125–133

6. **Crowe MJ, Bresnahan JC, Shuman SL, Masters JN, Beattie MS** 1997 Apoptosis and delayed degeneration after spinal cord injury in rats and monkeys. Nat Med 3:73–76

7. **Warden P, Bamber NI, Li H, Esposito A, Ahmad KA, Hsu CY, Xu XM** 2001 Delayed glial cell death following wallerian degeneration in white matter tracts after spinal cord dorsal column cordotomy in adult rats. Exp Neurol 168:213–224

8. **Negishi M, Katoh H** 2002 Rho family GTPases as key regulators for neuronal network formation. J Biochem 132:157–166

9. **Luo L** 2000 Rho GTPases in neuronal morphogenesis. Nat Rev Neurosci 1:173–180

10. **McKerracher L, Higuchi H** 2006 Targeting Rho to stimulate repair after spinal cord injury. J Neurotrauma 23:309–317

11. **Dubreuil CI, Winton MJ, McKerracher L** 2003 Rho activation patterns after spinal cord injury and the role of activated Rho in apoptosis in the central nervous system. J Cell Biol 162:233–243

12. **Yune TY, Lee JY, Jung GY, Kim SJ, Jiang MH, Kim YC, Oh YJ, Markelonis GJ, Oh TH** 2007 Minocycline alleviates death of oligodendrocytes by inhibiting pro-nerve growth factor production in microglia after spinal cord injury. J Neurosci 27:7751–7761

13. **Shaulian E, Karin M** 2002 AP-1 as a regulator of cell life and death. Nat Cell Biol 4:E131–E136

14. **Gupta S, Barrett T, Whitmarsh AJ, Cavanagh J, Sluss HK, Dérijard B, Davis RJ** 1996 Selective interaction of JNK protein kinase isoforms with transcription factors. EMBO J 15:2760–2770

15. **Kuan CY, Whitmarsh AJ, Yang DD, Liao G, Schloemer AJ, Dong C, Bao J, Banasiak KJ, Haddad GG, Flavell RA, Davis RJ, Rakic P** 2003 A critical role of neural-specific JNK3 for ischemic apoptosis. Proc Natl Acad Sci USA 100:15184–15189

16. **Okuno S, Saito A, Hayashi T, Chan PH** 2004 The c-Jun N-terminal protein kinase signaling pathway mediates Bax activation and subsequent neuronal apoptosis through interaction with Bim after transient focal cerebral ischemia. J Neurosci 24:7879–7887

17. **Herdegen T, Claret FX, Kallunki T, Martin-Villalba A, Winter C, Hunter T, Karin M** 1998 Lasting N-terminal phosphorylation of c-Jun and activation of c-Jun N-terminal kinases after neuronal injury. J Neurosci 18:5124–5135

18. **Kenney AM, Kocsis JD** 1998 Peripheral axotomy induces long-term c-Jun amino-terminal kinase-1 activation and activator protein-1 binding activity by c-Jun and junD in adult rat dorsal root ganglia in vivo. J Neurosci 18:1318–1328

19. **Yang DD, Kuan CY, Whitmarsh AJ, Rincón M, Zheng TS, Davis RJ, Rakic P, Flavell RA** 1997 Absence of excitotoxicity-induced apoptosis in the hippocampus of mice lacking the Jnk3 gene. Nature 389:865–870

20. **Hunot S, Vila M, Teismann P, Davis RJ, Hirsch EC, Przedborski S, Rakic P, Flavell RA** 2004 JNK-mediated induction of cyclooxygenase 2 is required for neurodegeneration in a mouse model of Parkinson's disease. Proc Natl Acad Sci USA 101:665–670

21. **Brecht S, Kirchhof R, Chromik A, Willesen M, Nicolaus T, Raivich G, Wessig J, Waetzig V, Goetz M, Claussen M, Pearse D, Kuan CY, Vaudano E, Behrens A, Wagner E, Flavell RA, Davis RJ, Herdegen T** 2005 Specific pathophysiological functions of JNK isoforms in the brain. Eur J Neurosci 21:363–377

22. **Li QM, Tep C, Yune TY, Zhou XZ, Uchida T, Lu KP, Yoon SO** 2007 Opposite regulation of oligodendrocyte apoptosis by JNK3 and Pin1 after spinal cord injury. J Neurosci 27:8395–8404

23. **Tang MX, Jacobs D, Stern Y, Marder K, Schofield P, Gurland B, Andrews H, Mayeux R** 1996 Effect of oestrogen during menopause on risk and age at onset of Alzheimer's disease. Lancet 348:429–432

24. **Bedard P, Langelier P, Villeneuve A** 1977 Oestrogens and extrapyramidal system. Lancet 2:1367–1368

25. **Soustiel JF, Palzur E, Nevo O, Thaler I, Vlodavsky E** 2005 Neuroprotective anti-apoptosis effect of estrogens in traumatic brain injury. J Neurotrauma 22:345–352

26. **Garcia-Segura LM, Azcoitia I, DonCarlos LL** 2001 Neuroprotection by estradiol. Prog Neurobiol 63:29–60

27. **Yune TY, Kim SJ, Lee SM, Lee YK, Oh YJ, Kim YC, Markelonis GJ, Oh TH** 2004 Systemic administration of 17β-estradiol reduces apoptotic cell death and improves functional recovery following traumatic spinal cord injury in rats. J Neurotrauma 21:293–306

28. **Yune TY, Park HG, Lee JY, Oh TH** 2008 Estrogen-induced Bcl-2 expression after spinal cord injury is mediated through phosphoinositide-3-kinase/Akt-dependent CREB activation. J Neurotrauma 25:1121–1131

29. **Lee SM, Yune TY, Kim SJ, Kim YC, Oh YJ, Markelonis GJ, Oh TH** 2004 Minocycline inhibits apoptotic cell death via attenuation of TNF-α expression following iNOS/NO induction by lipopolysaccharide in neuron/glia co-cultures. J Neurochem 91:568–578

30. **Iannotti C, Ping Zhang Y, Shields CB, Han Y, Burke DA, Xu XM** 2004 A neuroprotective role of glial cell line-derived neurotrophic factor following moderate spinal cord contusion injury. Exp Neurol 189:317–332

31. **Holstege JC, Kuypers HG** 1987 Brainstem projections to spinal motoneurons: an update. Neuroscience 23:809–821

32. **Eum WS, Kim DW, Hwang IK, Yoo KY, Kang TC, Jang SH, Choi HS, Choi SH, Kim YH, Kim SY, Kwon HY, Kang JH, Kwon OS, Cho SW, Lee KS, Park J, Won MH, Choi SY** 2004 In vivo protein transduction: biologically active intact pep-1-superoxide dismutase fusion protein efficiently protects against ischemic insult. Free Radic Biol Med 37:1656–1669

33. **Basso DM, Beattie MS, Bresnahan JC** 1995 A sensitive and reliable locomotor rating scale for open field testing in rats. J Neurotrauma 12:1–21

34. **Rivlin AS, Tator CH** 1977 Objective clinical assessment of motor function after experimental spinal cord injury in the rat. J Neurosurg 47:577–581

35. Merkler D, Metz GA, Raineteau O, Dietz V, Schwab ME, Fouad K 2001 Locomotor recovery in spinal cord-injured rats treated with an antibody neutralizing the myelin-associated neurite growth inhibitor Nogo-A. J Neurosci 21:3665–3673

36. Stirling DP, Khodarahmi K, Liu J, McPhail LT, McBride CB, Steeves JD, Ramer MS, Tetzlaff W 2004 Minocycline treatment reduces delayed oligodendrocyte death, attenuates axonal dieback, and improves functional outcome after spinal cord injury. J Neurosci 24:2182–2190

37. Beattie MS, Hermann GE, Rogers RC, Bresnahan JC 2002 Cell death in models of spinal cord injury. Prog Brain Res 137:37–47

38. Lee JY, Chung H, Yoo YS, Oh YJ, Oh TH, Park S, Yune TY 2010 Inhibition of apoptotic cell death by ghrelin improves functional recovery after spinal cord injury. Endocrinology 151:3815–3826

39. Gu C, Casaccia-Bonnefil P, Srinivasan A, Chao MV 1999 Oligodendrocyte apoptosis mediated by caspase activation. J Neurosci 19:3043–3049

40. Yamashita T, Higuchi H, Tohyama M 2002 The p75 receptor transduces the signal from myelin-associated glycoprotein to Rho. J Cell Biol 157:565–570

41. Sung JK, Miao L, Calvert JW, Huang L, Louis Harkey H, Zhang JH 2003 A possible role of RhoA/Rho-kinase in experimental spinal cord injury in rat. Brain Res 959:29–38

42. Harrington AW, Kim JY, Yoon SO 2002 Activation of Rac GTPase by p75 is necessary for c-jun N-terminal kinase-mediated apoptosis. J Neurosci 22:156–166

43. Jurewicz A, Matysiak M, Tybor K, Selmaj K 2003 TNF-induced death of adult human oligodendrocytes is mediated by c-jun NH2-terminal kinase-3. Brain 126(Pt 6):1358–1370

44. Pirianov G, Brywe KG, Mallard C, Edwards AD, Flavell RA, Hagberg H, Mehmet H 2007 Deletion of the c-Jun N-terminal kinase 3 gene protects neonatal mice against cerebral hypoxic-ischaemic injury. J Cereb Blood Flow Metab 27:1022–1032

45. Yin KJ, Kim GM, Lee JM, He YY, Xu J, Hsu CY 2005 JNK activation contributes to DP5 induction and apoptosis following traumatic spinal cord injury. Neurobiol Dis 20:881–889

46. David S 2002 Recruiting the immune response to promote long distance axon regeneration after spinal cord injury. Prog Brain Res 137:407–414

47. Kerschensteiner M, Schwab ME, Lichtman JW, Misgeld T 2005 In vivo imaging of axonal degeneration and regeneration in the injured spinal cord. Nat Med 11:572–577

48. Lehmann M, Fournier A, Selles-Navarro I, Dergham P, Sebok A, Leclerc N, Tigyi G, McKerracher L 1999 Inactivation of Rho signaling pathway promotes CNS axon regeneration. J Neurosci 19:7537–7547

49. Dergham P, Ellezam B, Essagian C, Avedissian H, Lubell WD, McKerracher L 2002 Rho signaling pathway targeted to promote spinal cord repair. J Neurosci 22:6570–6577

50. Dillon ST, Feig LA 1995 Purification and assay of recombinant C3 transferase. Methods Enzymol 256:174–184

51. Yune TY, Lee JY, Jiang MH, Kim DW, Choi SY, Oh TH 2008 Systemic administration of PEP-1-SOD1 fusion protein improves functional recovery by inhibition of neuronal cell death after spinal cord injury. Free Radic Biol Med 45:1190–1200

52. Hawkins MB, Thomas P 2004 The unusual binding properties of the third distinct teleost estrogen receptor subtype ERβa are accompanied by highly conserved amino acid changes in the ligand binding domain. Endocrinology 145:2968–2977

53. Fournier AE, Takizawa BT, Strittmatter SM 2003 Rho kinase inhibition enhances axonal regeneration in the injured CNS. J Neurosci 23:1416–1423

54. Sawada H, Ibi M, Kihara T, Urushitani M, Akaike A, Shimohama S 1998 Estradiol protects mesencephalic dopaminergic neurons from oxidative stress-induced neuronal death. J Neurosci Res 54:707–719

55. Culmsee C, Vedder H, Ravati A, Junker V, Otto D, Ahlemeyer B, Krieg JC, Krieglstein J 1999 Neuroprotection by estrogens in a mouse model of focal cerebral ischemia and in cultured neurons: evidence for a receptor-independent antioxidative mechanism. J Cereb Blood Flow Metab 19:1263–1269

56. Dubal DB, Shughrue PJ, Wilson ME, Merchenthaler I, Wise PM 1999 Estradiol modulates bcl-2 in cerebral ischemia: a potential role for estrogen receptors. J Neurosci 19:6385–6393

57. Honda K, Sawada H, Kihara T, Urushitani M, Nakamizo T, Akaike A, Shimohama S 2000 Phosphatidylinositol 3-kinase mediates neuroprotection by estrogen in cultured cortical neurons. J Neurosci Res 60:321–327

58. Dubal DB, Kashon ML, Pettigrew LC, Ren JM, Finklestein SP, Rau SW, Wise PM 1998 Estradiol protects against ischemic injury. J Cereb Blood Flow Metab 18:1253–1258

59. Behl C, Skutella T, Lezoualc'h F, Post A, Widmann M, Newton CJ, Holsboer F 1997 Neuroprotection against oxidative stress by estrogens: structure-activity relationship. Mol Pharmacol 51:535–541

60. Alkayed NJ, Goto S, Sugo N, Joh HD, Klaus J, Crain BJ, Bernard O, Traystman RJ, Hurn PD 2001 Estrogen and Bcl-2: gene induction and effect of transgene in experimental stroke. J Neurosci 21:7543–7550

61. Singer CA, Figueroa-Masot XA, Batchelor RH, Dorsa DM 1999 The mitogen-activated protein kinase pathway mediates estrogen neuroprotection after glutamate toxicity in primary cortical neurons. J Neurosci 19:2455–2463

62. Lu A, Ran RQ, Clark J, Reilly M, Nee A, Sharp FR 2002 17-β-estradiol induces heat shock proteins in brain arteries and potentiates ischemic heat shock protein induction in glia and neurons. J Cereb Blood Flow Metab 22:183–195

63. Jiménez B, Arends M, Esteve P, Perona R, Sánchez R, Ramón y Cajal S, Wyllie A, Lacal JC 1995 Induction of apoptosis in NIH3T3 cells after serum deprivation by overexpression of rho-p21, a GTPase protein of the ras superfamily. Oncogene 10:811–816

64. Aznar S, Lacal JC 2001 Rho signals to cell growth and apoptosis. Cancer Lett 165:1–10

65. Marinissen MJ, Chiariello M, Tanos T, Bernard O, Narumiya S, Gutkind JS 2004 The small GTP-binding protein RhoA regulates c-jun by a ROCK-JNK signaling axis. Mol Cell 14:29–41

66. Coffey ET, Smiciene G, Hongisto V, Cao J, Brecht S, Herdegen T, Courtney MJ 2002 c-Jun N-terminal protein kinase (JNK) 2/3 is specifically activated by stress, mediating c-Jun activation, in the presence of constitutive JNK1 activity in cerebellar neurons. J Neurosci 22:4335–4345

67. Ferrer I, Olive M, Ribera J, Planas AM 1996 Naturally occurring (programmed) and radiation-induced apoptosis are associated with selective c-Jun expression in the developing rat brain. Eur J Neurosci 8:1286–1298

68. Herdegen T, Fiallos-Estrada CE, Schmid W, Bravo R, Zimmermann M 1992 The transcription factors c-JUN, JUN D and CREB, but not FOS and KROX-24, are differentially regulated in axotomized neurons following transection of rat sciatic nerve. Brain Res Mol Brain Res 14:155–165

69. Jenkins R, Tetzlaff W, Hunt SP 1993 Differential expression of immediate early genes in rubrospinal neurons following axotomy in rat. Eur J Neurosci 5:203–209

70. Raghupathi R, McIntosh TK, Smith DH 1995 Cellular responses to experimental brain injury. Brain Pathol 5:437–442

71. Kobori N, Clifton GL, Dash P 2002 Altered expression of novel genes in the cerebral cortex following experimental brain injury. Brain Res Mol Brain Res 104:148–158

72. Vasudevan H, Xiang H, McNeill JH 2005 Differential regulation of insulin resistance and hypertension by sex hormones in fructose-fed male rats. Am J Physiol Heart Circ Physiol 289:H1335–H1342

73. Bulun SE, Sebastian S, Takayama K, Suzuki T, Sasano H, Shozu M 2003 The human CYP19 (aromatase P450) gene: update on physiologic roles and genomic organization of promoters. J Steroid Biochem Mol Biol 86:219–224